Application of seismic refraction and tomography methods to the assessment of the Sivaki dam site

Fariba Kargaranbafghi [1] *, Farshad Ghalamzan [1]

[1] *Department of Geology, Yazd University, Safaieh, 89195-741 Yazd, Iran*
*Corresponding author E-mail: fkargaran@yazd.ac.i

Abstract

The Sivaki Dam site located near Sepidar Road, approximately 50 km southwest of Yasuj City was selected for geophysical investigations. The objective of the study was to detect low velocity zones potentially liable to water infiltration or leakage and to evaluate the dynamic properties of subsurface materials. The study applied a combination of shallow seismic refraction profiling and seismic tomography methods. The P-wave velocity in most parts obtained from seismic tomography investigation is less than 3km/s. This velocity corresponds to the high Lugeon number (> 10), which is the indicator of high permeability of dam foundation. Based on the seismic tomography and Lugeon section, at the right abutment, rock mass quality improves towards deeper parts but because of high Lugeon value need for grouting at deep levels. According to Iranian-2800, seismic building code the upper layer has average shear velocity values that range from 375 m/s to 750 m/s and classified as hard soil and mixtures of sands, gravels and clays. According to the national earthquake hazard reduction program (NEHRP) provisions scheme, the Sivaki dam site is preliminarily classified into two site classes (B and C).

Keywords: *Seismic Refraction; Seismic Tomography; Shear Wave; Sivaki Dam; Waves Velocity*.

1. Introduction

The Sivaki Dam is an earth dam with clay core that is constructed on the Sepidar River at the 50km of the Yasuj city. The study area is located on the Sisakht 1:100000 map in the latitude 30˚37' and longitude 51˚19'. The study area is located between the High Zagros and Zagros Folded Belt. The outcrops in the area are often Asmari limestone. The right and left abutment of the dam site are cream limestone with the Asmari formation Interlayers. In the high altitude of the left abutment contains gypsum, red marl and marly limestone of the Gachsaran formation. In the depth of the site consists of mainly marl, limestone shale and marly limestone of the Pabdeh formation [1]. Bedrock consists of the young trusts and alluvial-fans. The main structural features of the area belongs to major structures of the Zagros that constructed on the Alpine orogeny in the Pliocene and Pleistocene [2]. In reference to the calcareous of the dam site and the possibility of karstification of the Asmari formation and saving in geotechnical studies, at the beginning seismic studies in the right abutment of Sivaki dam site by boundary reflection method was conducted in two cross sections of A-A' and B-B' and also seismic tomography method done in two boreholes BS5 and BS6. The target of this study is to obtain change of attenuation and velocity of the waves to know subsurface structures. Pressure and shear wave velocity were calculated in the study boreholes and consequent catch geotechnical parameters [3], [4]. These parameters have extensive application and important in the engineering tasks. Lugeon test is used for determination of leakage from the foundation and abutments of the dam site [5]. The experiment results can only check the area close to borehole. If the joints and discontinuities didn't cut the borehole, the data will not be enough accurate. The seismic tomography survey the permeability an extensive area easy and with lower cost [6]. Therefore in the early stage, the seismic tomography studies in the boreholes is carried out before the extensive excavation in the area. In this study, seismic data processing done by Geotomo 5.1, Ras24 2.15, Reflexw 5.05 and Surfer 7.0 softwares.

2. Method of geophysical studies at the site

2.1. Seismic refraction theory

Boundary seismic reflection is one of the most common methods for geophysical explorations. Low cost, simple application and diverse interpretation methods have raised the application of this method in the study of sites and other engineered structures [7, 8]. In this method, measurements are carried out by creation of seismic wave by artificial energy sources (explosion or mechanical) in one point and determination of the arrival time of direct, reflected and refracted waves to the layers interface equipped with a series of receptors located in a direct line on the land surface (Figure 1).
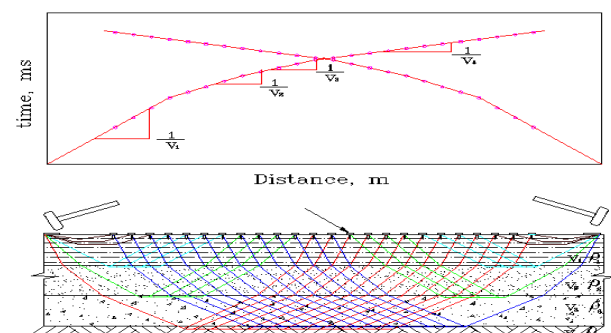

Fig. 1: Transitional Failover Seismic Operations with Wave Routes [9].

By release of energy in the earth up to a specific distance, called cross-over distance, the first received wave of the receptors is the direct wave moving at the speed of v1 whose time of travel can be determined as [10], [11]:

$$t_1 = X/V_1 \qquad\qquad (1)$$

T1 is the arrival time of the direct wave and X represents the distance between the wave source and receiver and V_1 is the wave velocity in the layer's surface. From this distance, the first received wave is the boundary refracted wave, which moves in the second layer with the wave velocity after being reflected by the critical angle from the layer one and two interface. If the wave propagation velocity increases by increase of depth, the time-distance equation for these waves in a simple horizontal two-layer model will be [12, 13]:

$$t_2 = \frac{X}{V_2} + \frac{2H_1 Cos\theta}{V_1} \qquad ; \quad V_2 > V_1 \qquad (2)$$

Where, H_1 is the first layer thickness (superficial layer), is the critical angle, V_1 and V_2 represent propagation velocities in first and second layers, respectively; and t_2 is the arrival time of the refracted wave. By plotting the two equations in time-distance coordinate, it can be seen that wave propagation velocity in first medium and second medium can be obtained from the inverse slopes of the direct waves and boundary refracted waves, respectively. As natural layers are not always horizontal and direct, and they mostly have slope and roughness, for complete coverage along the profile, the measurements will be repeated in specific intervals and the wave propagation to the earth will be carried out. Results of this operation can be obtained by one of the conventional interpretation methods based on the desired accuracy and number of layers, velocity and layer thickness beneath each of the receivers (geophones) [14].

2.2. Theory of intrinsic methods

2.2.1. Surface to depth method (down-hole)

In this method, the seismic wave source is on the surface near the borehole and the receiver is placed in the borehole scanning the entire borehole length. This method is applicable in noisy places as the noise will reduce by receiver getting further in depth of the borehole, therefore the quality of records will be enhanced (Figure 2) [15].
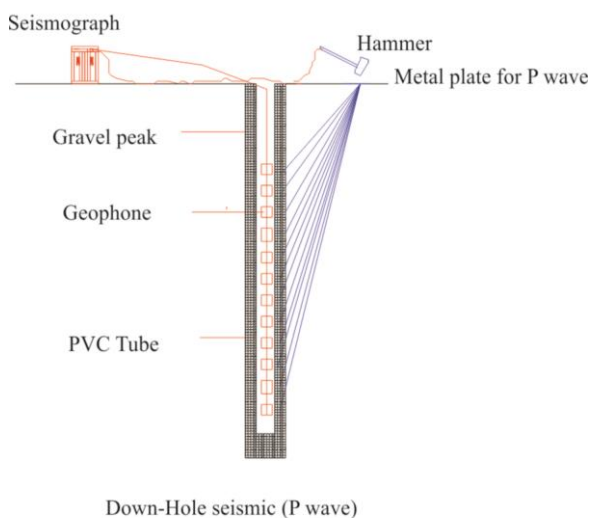

Down-Hole seismic (P wave)

Fig. 2: A Sequence of Seismic Operations in Well, Surface to Depth [15].

2.2.2. Depth to surface method (up-hole)

In this method, the receiver is on the surface near the borehole and the seismic wave source is placed in the borehole scanning the

entire borehole length. As the receiver is on the surface, it can be controlled easier. This control is very difficult and more time-consuming in inside-well methods.

2.2.3. Vertical seismic profile method (vertical seismic profiling)

This is similar to down-hole method but the seismic wave source will be placed in different distances from the borehole opening and the receiver will scan all the borehole depth. By this method, the average velocity of layers between the transmitter and receiver can be obtained; therefore, the existing layers can be differentiated by placing the receiver in different depths [15].

2.2.4. Tomography method depth to depth or between walls (cross whole tomography)

In this method, two boreholes are drilled with a specific distance from each other. Then the wave receiver will be placed in one borehole and the seismic wave source will be located in the other. All these elements simultaneously scan all depths of the borehole (Figure 3). As both receiver and source are placed inside the borehole, the seismic wave velocity can be obtained even in low-thickness layers [15]. This is an efficient method in detection of abnormalities such as crushed ventures and holes and can give an overall estimation of rock quality.

Tomography experience with sparker seismic source is a non-destructive test in which a hydrophone fiber will be placed in one borehole and a seismic wave source will be located in another. Sound waves will pass the section and each beam will pass the distance in a specific time (Figure 4). If the studies cross section is divided into different cells (Figure 5), each beam will pass different blocks and at each block it will pass a specific distance. For instance in figure 5, MN beam passes different cells and the passed distance in ij cell is about S_{MNij}. Generally, following equation holds between the wave arrival time, its velocity and distance in the cells in the path of the wave beam [16]:

$$T_{MN} = \sum \frac{S_{mnij}}{V_{ij}} \qquad (3)$$

In which, T_{MN} is the time passed by MN beam and V_{ij} represents the seismic waves velocity in ij cell. To solve this equation, simulation methods are used. First, a mean velocity is considered for all the cells. Then by regression analysis and trial and error technique, the cells' velocity will be changed till the minimum RMS is achieved. Finally, iso-velocity curves will be plotted by considering the velocity of each cell to their center. By means of these curves, high and low-speed zones can be identified. The regions with lower velocities will be considered as crushed, fractured or porous zones depending on their shapes. Regions with higher velocities will be attributed to denser and intact rocks.
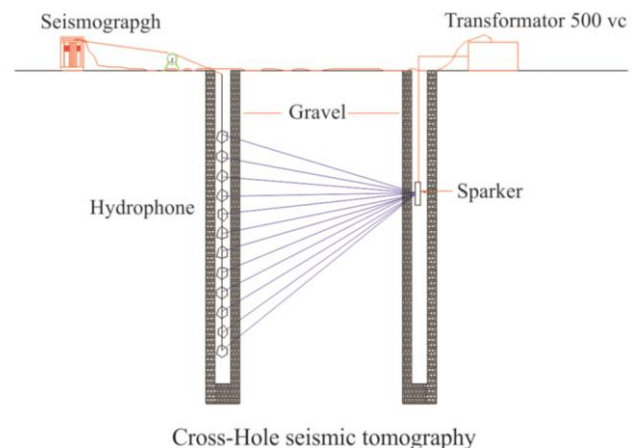

Cross-Hole seismic tomography

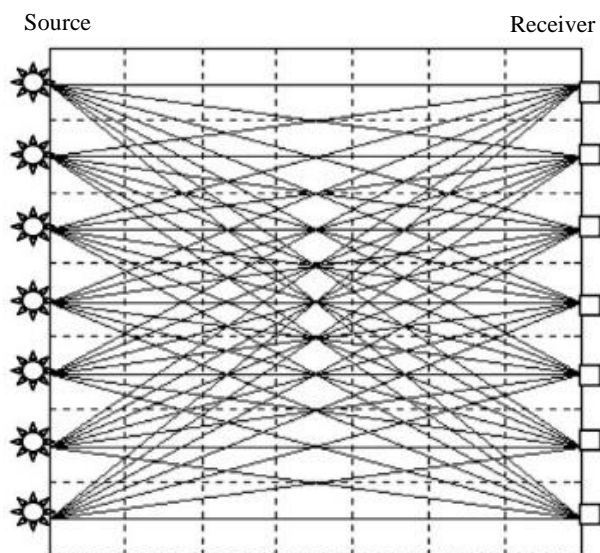**Fig. 3:** A Seismic Operation of Tomography between Boreholes [16].

Fig. 4: Seismic Wave Paths in Seismic Tomography [17].
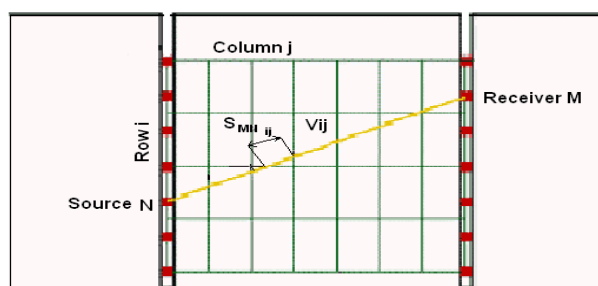

Fig. 5: Cell Division in Seismic Tomography.

3. The velocity values of various materials and dynamic parameters

In all the construction projects, the elastic moduli of the region components will have the necessary insight to the engineers. Wave velocity varies in different formations and is the function of type, density, porosity, water content and elastic properties of the environment in which the wave is released. Approximated values of the shear and pressure waves velocity in some components of land layers are listed in table 1. These quantities can be calculated by density and velocity of the shearing and pressure waves in different materials in addition to geotechnical experiments. Therefore, to obtain the mentioned parameters in a region, it is necessary to consider some profiles for shearing wave velocity (V_s) determination in addition to measurement of pressure wave velocity (V_p).

Table 1: Approximate Speed of Compression and Shear Waves in Some Materials [18], [19].

Materials	Density (gr/cm^3)	V_p (m/s)	V_s (m/s)
Water	1	1500	-
Sand & gravel	1.5 - 2	500-1900	300-900
Silt & clay	1.3 – 1.7	300-1900	100-500
Marl	1.3 – 1.7	300-1900	100-500
Gypsum	1.8 – 2.2	1700-3000	600-1500
Hard lime	2.5 – 2.7	3000-6500	1500-3500
Weathered granite	2 – 2.7	1000-3000	500-1500
Healthy granite	2.6 – 2.8	3000-6000	1500-3000
Silt	2.7	5000-7000	3000-3800

4. Seismic studies results

4.1. Seismic study results by border failure at Sivaki site

Seismic studies by boundary reflection method was conducted in two cross sections of A-A' and B-B' whose locations are depicted in figure 6. Descriptions of the recorded mappings are also listed in table 2. After data processing, first arrival time of each beam was derived and the seismic wave's velocities were calculated by tomographic boundary reflection simulation of each cell. Iso-velocity curves of pressure waves were plotted according to wave velocity in each cell. Then cross section of the real layers were plotted by interpretation of these curves, as the underground water level is more than 20 m in this region, it is possible to plot the iso-velocity cross section of the shear wave by consideration of pressure to shearing wave ratio of 1/9.
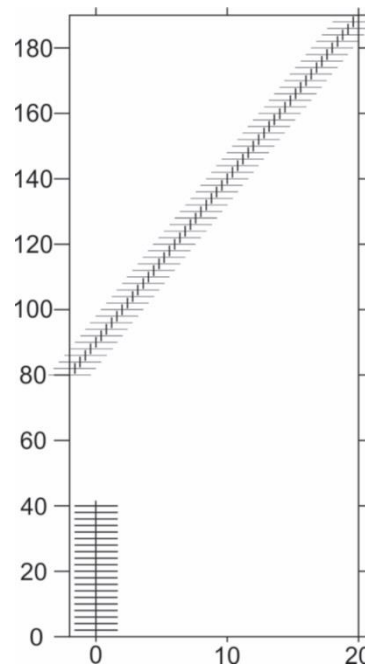

Fig. 6: Position of the Boundary Refraction Profiles on Sivaki Site.

Table 2: Description of the Number of Mapped Boundary Refraction Profiles on Sivaki Site.

Description of Operation	Number of receivers	Number of shots per line	Number of withdrawal lines	Number of mappings
Cross border in section 1	7	5	3	105
Cross border in section 2	7	7	8	392
Total mapping			497	

A-A' section is 40 meter long at the distance of 20 m from the borehole initiated from 2040 m and continued to 2050 m. Iso-velocity curves of pressure seismic waves for this cross section was plotted (Figure 7, up). Also, shearing waves velocity was calculated from pressure waves velocity for A-A' section (Figure 7, down). Debris layers and weathered rocks can be observed in upper part of this section the thickness of this layer is 3-8 m. In central parts and in 15- to 35-m distances at 4- to 20-m depth, a relatively intact rockmass can be seen. At distance of 10 m from the beginning of the profile at 2030 m, a mass with lower seismic wave velocity can be observed which can be attributed to a crushed zone, probably a fault.
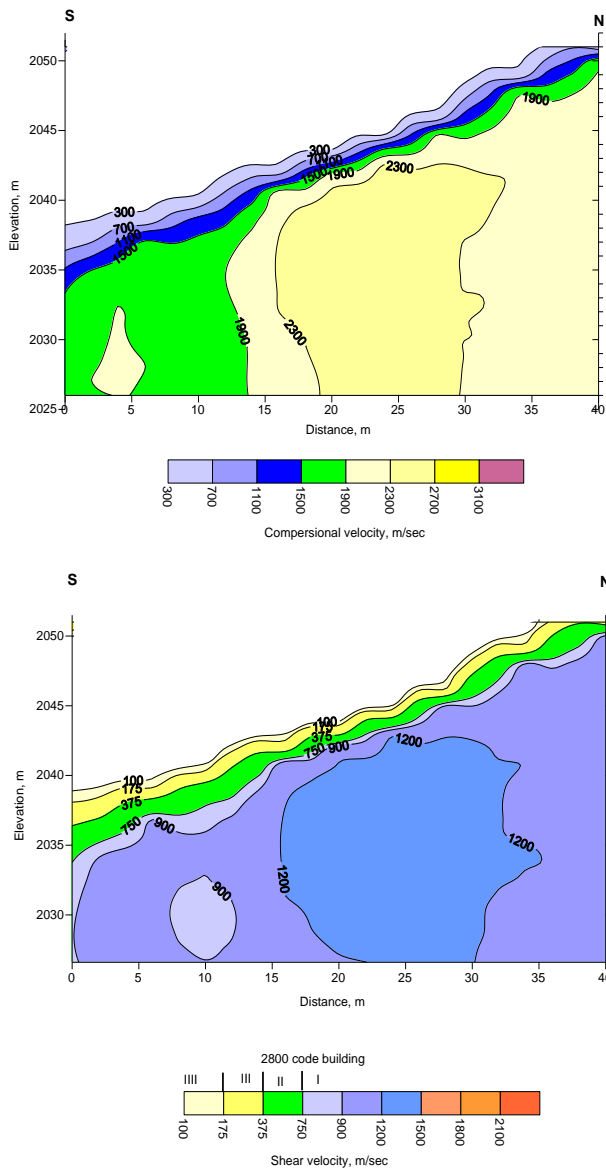
Fig. 7: Seismic Section A-A, Compression Wave Section (Up), Shear Wave Section (Lower).

B-B' section is 94 meters long recorded at elevation of 2065 to 2075 m. Iso-velocity curves of pressure seismic waves for this cross section was plotted (Figure 8, up). Also, real layers' cross sections were plotted by interpreting the iso-velocity curves (Figure 8, down). Debris layers and weathered rocks can be observed in upper part of this section the thickness of this layer is about 10 m in southern parts. In central parts of profile, the thickness of debris and weathered rocks reduced to lower than 5 m from 30- to 70-meter distance. In this part, a relatively intact rock can be seen in 4-18 m depth. In northern part of the profile and at 70- to 90-meter distance from the southern part, the velocity of shearing waves was reduced to 375 m/s in 0- to 5-meter distance which can be sign of weak sedimentation rocks.
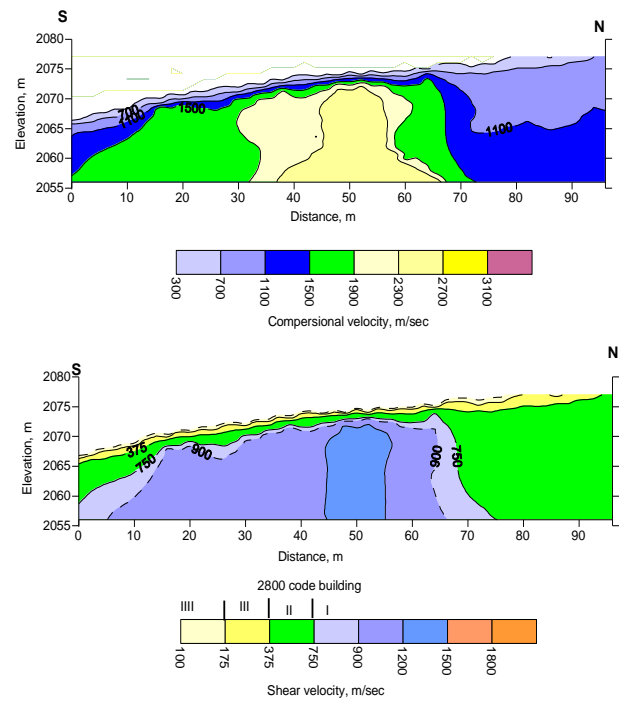

Fig. 8: Seismic Section B-B, Compression Wave Section (Up), Shear Wave Section (Lower).

4.2. Seismic study results by tomography method on Sivaki site

At Sivaki dam site, two boreholes were drilled. BS5 was drilled with 30-degree incline from the vertical direction and BS6 was drilled vertically. Receivers, seismic wave source and the site of the dam are shown in figure 9. Details of the recorded mappings in each method are listed in table 3. After data processing, the first arrival time of each beam was derived and plotted by simulation of iso-velocity curves of pressure seismic waves (Figure 10). Based on a local scale, the rocks with pressure wave velocity more than 3000 m/s are related to resistant and intact lime rocks and those with velocity of 2400 to 3000 m/s can be attributed to medium-resistant rocks with cracks. Rocks whose passing velocities are lower than 2400 m/s are classified as weak and weathered rocks. Ultra-aerated rocks and sand have velocities in the range of 500-1500 m/s [18, 19]. In central part of A-A' section (Figure 10), from the depth of 5 to 40 m, the variation trend of waves velocity revealed the existence of low-resistance rocks. The thickness of debris layer varied from 3 to 12 m. the variation trend of seismic wave velocities at the north of the profile indicated a fracture.
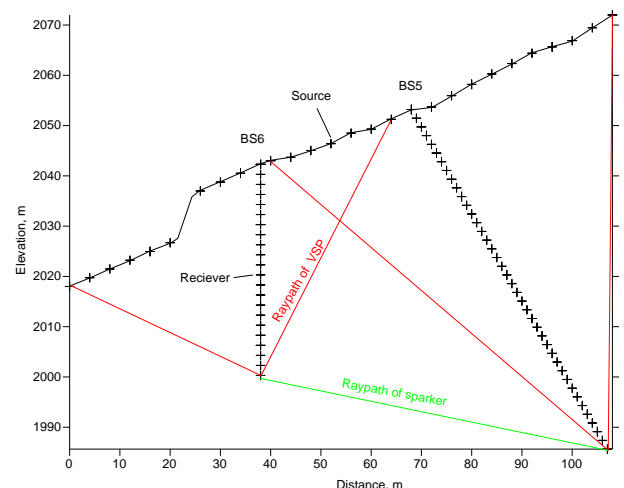

Fig. 9: VSP Separator Sprinkler Location and Sparker and Receivers on Sivaki Site.

Table 3: Describes the Number of Digits Taken on Sivaki Site

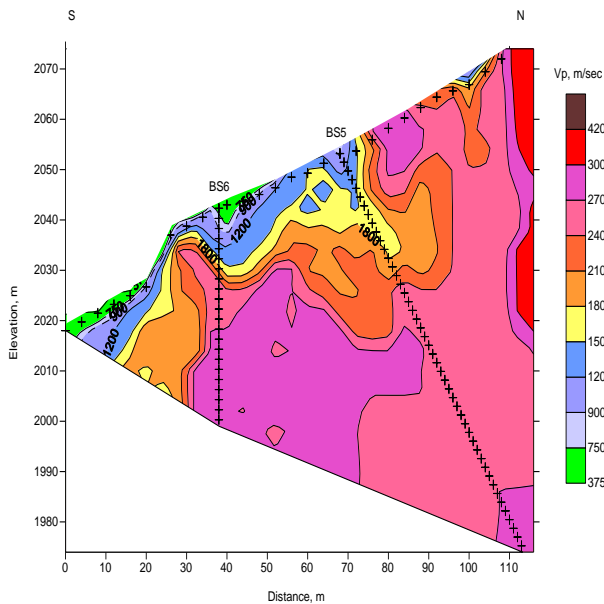| Description of Operation	Number of Shots	Number of receiver depth	Number of mappings
VSP in BS6	16	21	336
VSP in BS5	17	43	731
Tomography between BS5-BS6	30	21	630
Total mapping			1697

Fig. 10: Seismic Section A-A, Cross Section Velocity of Condensation Wave on Sivaki Site.

5. Integration of geophysical and geotechnical results

In this study, geotechnical parameters and dynamic properties were investigated for near-surface soils (up to 30 meter depth) at the right side of Sivaki dam by the help of pressure and shear wave's velocity. Wave velocity differs in different geological layers and is a function of type, density, porosity, water content and elastic properties of the environment. In construction projects such as dam construction, dynamic elastic moduli of the components of the site region can provide the engineers with proper insight. Dynamic parameters can be also obtained by use of density and wave velocity. The density can be determined from pressure waves. Abutments permeability is another important parameter in dam construction which can result in water scape or dam destruction. Permeability test of Lugeon is generally carried out in the boreholes and their results will be adapted with the wave velocity in the same borehole. Then a local relation can be obtained between the wave velocity and Lugeon number. Finally, Lugeon number could be obtained for the other regions.

5.1. The relationship between the compressive and shear wave velocity

Due to difference of pressure wave with shear waves, they would be differently affected by elastic properties of the rock. Therefore, if they can be simultaneously investigated in a single rock sample, valuable information could be obtained. Due to difficulties in collecting data of shearing seismic wave, their information can be derived from the information concerning pressure waves. V_p/V_s ratio of each region can be obtained from the empirical equations (between pressure and shearing waves. It is better to calculate these equations for each region individually. V_p/V_s ratio is one of the important dynamic parameter. Numerous empirical equations have been presented for this ratio; among which Domenico equation (1984) can be mentioned which presented a curve for lime rock (Figure 11). In this study, empirical curves was employed

according to the layers condition and geotechnical tests (Figure 12). Maximum velocity of pressure wave for dense lime layers is about 3000 m/s which will result in minimum V_p/V_s ratio (about 1.8). For weak alluvial layers, this velocity is about 350 m/s which will give rise to maximum V_p/V_s ratio (about 2.1) [20], [21]. Regarding these findings, iso-velocity cross section of shear wave was plotted in Sivaki dam site (Figure 13). Shear wave velocity is important and dynamic parameters can be obtained by that. In classification of land layers according to shear wave's average velocity up to the depth of 30 m, the building design regulation of Iran called regulation 2800 and national earthquake hazard reduction program [22] were used (Table 4). Average velocity of shearing wave in debris is about 375-750 m/s; the alluvial thickness of the region is less than 30 m. therefore, the studied site can be classified as the type I based on regulation 2800. In the studied site, the shearing wave's velocity rarely exceeded 1500 m/s up to the depth of 30 m (of exceeding of pressure wave from 2600 m/s); hence, there is no ultra-hard rock in the dam site. Based on NEHRP regulation, the studied region can be classified as rank B (rock).
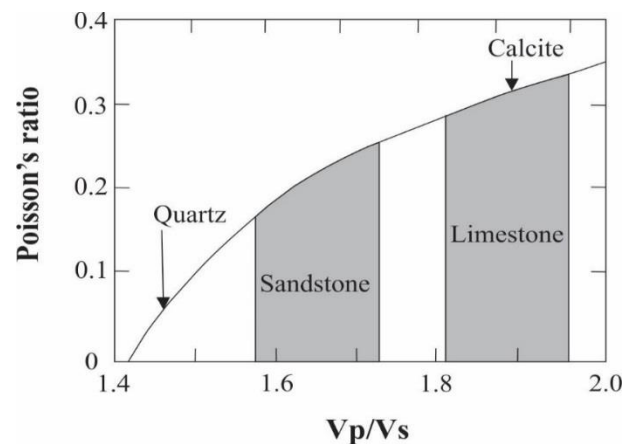

Fig. 11: Relationship between Density and Poisson's Ratio and Compression Wavelength Vp/vs in Limestone and Sandstone Rock [23].
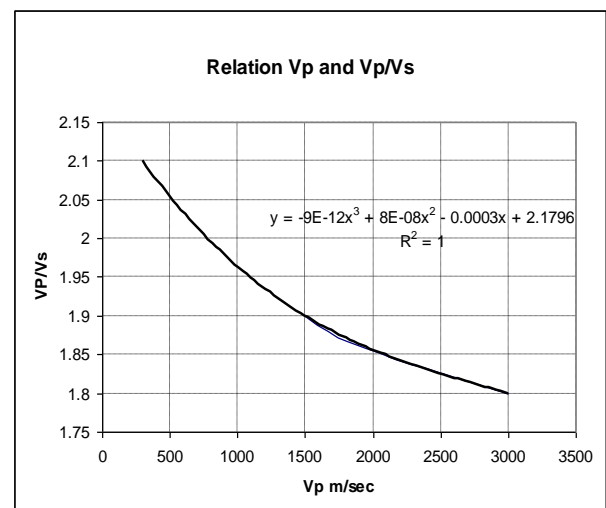

Fig. 12: The Relationship between Compression Wave and Ratio Compressive and Shear Wave Speed in This Study.
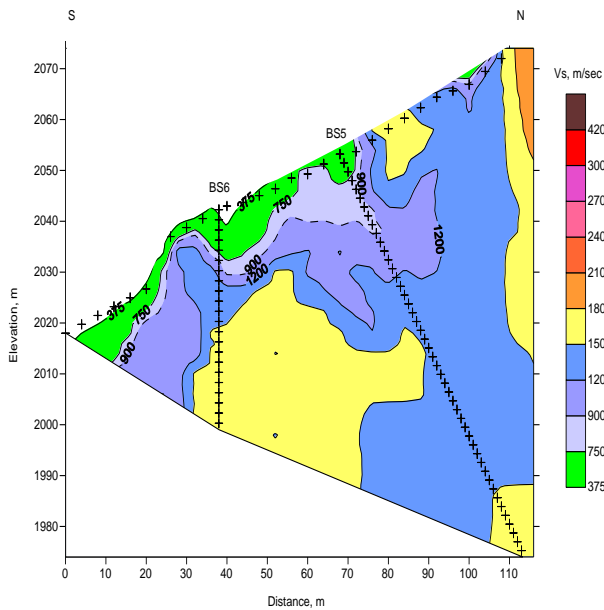
Fig. 13: Seismic Section A-A, the Shear Wave Velocity Map on Sivaki Site.

Table 4: Classification of Sites in Terms of Soil and Stone [22].

Category	Average of shear wave velocity higher than 100 FT (30 m)	Standard penetration speed	Stone and soil category
A	5000ft/sec(>1500m/sec)	Not applicable	Hard rock
B	2500 تا 5000ft/sec (760 تا1500 m/sec)	Not applicable	Rock
C	1200 تا2500ft/sec (360 تا 760 m/sec)	>50	High-density soil and soft rock
D	600 تا1200ft/sec (180 تا360 m/sec)	15 تا50	Hard soil
E	<600ft/sec (<180 m/sec)	<15	Soft soil
F	Soil susceptible to seizure failure, including soil with high plastics and fluidity	Not applicable	A specific category that requiring geotechnical evaluation

5.2. The relationship between density and condensation velocity

By increase of density, by assuming constant layer type, the velocity of pressure wave will also increase. The maximum velocity of pressure wave is 3000 m/s for lime layers for which maximum density of 2.5 g/cm3 was considered. For weak alluvial layers, the pressure wave velocity is 350 m/s for which the minimum density of 1.7 g/cm^3 was considered [19, 24]. The relationship between the pressure wave velocity and applied density is depicted in figure 14. By following formula, the density can be calculated according to the velocity of pressure wave, in following equation, if density is denoted by ρ (in g/cm^3) and pressure wave velocity (v_p) is in m/s, the value of a will be considered 0.31 [25, 26].

$$\rho = aVp0.25 \tag{4}$$

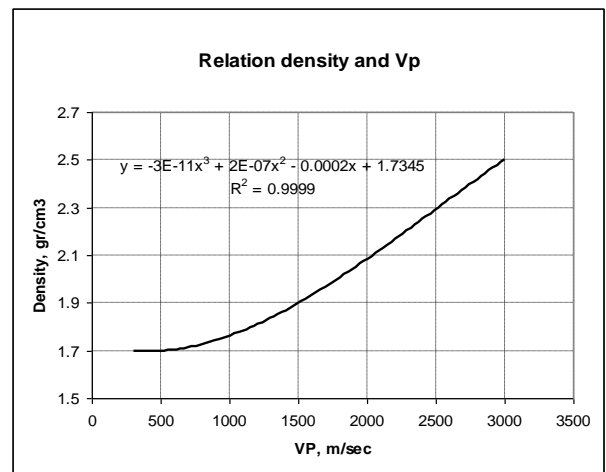$$a = 0.31 \ m/s \tag{5}$$

Fig. 14: The Relationship between Compression Wavelength and Density Used in This Study.

5.3. Relationship between the velocity of compression waves and permeability

So far, numerous studies have addressed the relationship between permeability and seismic wave velocities in the rock. Barton (2006) studied hard rocks and showed that increase of pressure wave velocity will decrease the Lugeon number. In porous rocky mass, crushed pores will increase permeability and decrease the seismic velocity. Studies have revealed the inverse relationship of pressure wave and Lugeon number [28]. In Barton equation, a relationship was presented between Lugeon number and pressure wave in hard rocks:

$$L=10(3.5-V_P) \tag{6}$$

Where, L is Lugeon number and V_p represents the velocity of pressure wave. Based on Houlsby (1990) studies, Lugeon numbers higher than 5 show potential of leakage in the site and that need to be sealed [30]. In Sivaki dam site, first the relationship between the velocity of pressure wave and Lugeon number was plotted (Figure 15). Then, iso- Lugeon section of A-A' was plotted by means of the obtained equations and software (Figure 16). Maximum velocity of pressure wave in the site was 3000 m/s corresponding to a region with Lugeon number of 10. In a very small region of the site, Lugeon numbers less than 10 were observed which are marked by yellow color. In central part of A-A' section, Lugeon number started from 120 in alluvium and reached to 25 at the depth of 40 m. In deeper regions, Lugeon number varied from 25 to 10. Seismic studies showed that rock quality increased with increase of depth but the Lugeon number was more than 10 showing the risk of water leakage even in deeper parts. Therefore sealing is needed even in deep parts. Results of new studies of Lugeon test for determination of leakage from the foundation and abutments of Sivaki dam site are in good agreement with Lugeon numbers obtained from tomographic seismic methods.
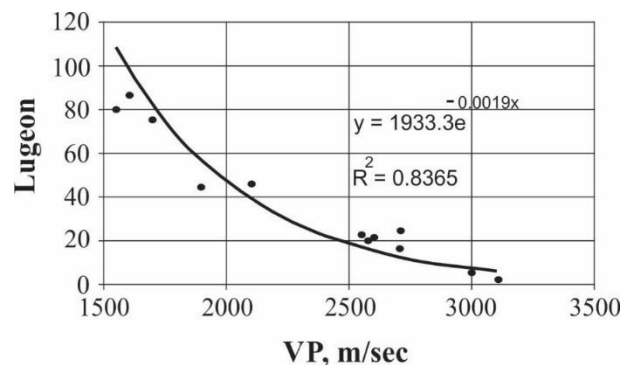

Fig. 15: The Relationship between Condensation Wave Speed and Lugeon on Sivaki Site.
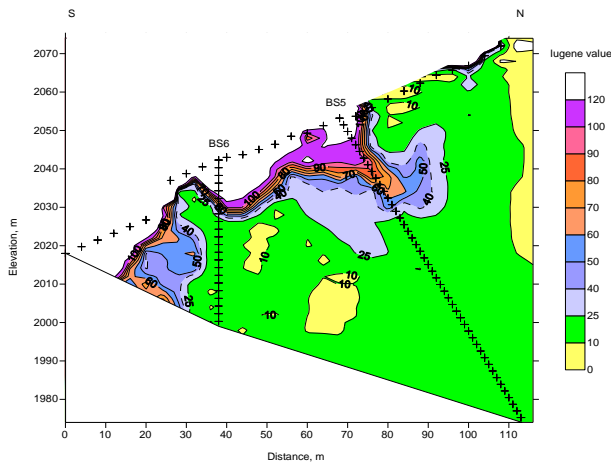
Fig. 16: The Section of the Lugeon Value of Sivaki Site.

5.4. Determine the dynamic parameters used on the site

Geophysical methods are used for assessment of the engineering properties of the rocks. These properties include Young's modulus, shear modulus, Bulk modulus and Poisson coefficient which are called elastic constants of the rock. Rock density can be also estimated by seismic velocities. To determine elastic constants, it is required to measure the velocities of pressure and shearing wave. Dynamic parameters can be calculated by estimation of density, pressure and shearing wave velocities. These moduli are for very small strains. For larger strain values, other tests such as cyclic three-axis method, resonance column, pressure-meter and planar loading should be employed. Results of seismic tests can be compared with the other tests' results. The relationship between the dynamic parameters, velocity of pressure wave, shearing wave and density can be calculated by following equations [31 34]

$$\upsilon = \frac{(\frac{V_p}{V_s})^2 - 2}{2[(\frac{V_p}{V_s})^2 - 1]} \quad \text{(Poisson's ratio)} \tag{7}$$

$$(\frac{V_p}{V_s})^2 = \frac{2 - 2\upsilon}{1 - 2\upsilon} \quad \text{(Ratio of compression waves to shear speed)} \tag{8}$$

$$G = \rho . V_s^2 \text{ (Shear modulus)} \tag{9}$$

$$E = 2G(1 + \upsilon) \text{ (Young's modulus)} \tag{10}$$

$$K = \frac{1}{3} . \frac{E}{1 - 2\upsilon} \text{ (Balk modulus)} \tag{11}$$

In above equations, the velocity of pressure and shearing waves are represented by V_p and V_s, respectively. Density is shown by ρ and Poisson ration was denoted by υ. Poisson ratio is approximately equal to 0.15-0.25 for igneous rocks, 0.16-0.35 for sedimentation rocks and 0.1-0.49 for soil. Elasticity modulus (young), shear modulus and bulk modulus maps were plotted for Sivaki dam site (Figures 17-19). Elastic modulus depends on the velocity of pressure and shearing waves, since the pressure wave velocity depends on humidity percentage and water content of the rock. The calculated elastic modulus will be more than elastic moduli calculated for dry layers. The map does not show iso-Young modulus in A-A' section (Figure 17) in contrary to shear and bulk moduli and in general, it shows less similarity with the maps of pressure and shearing waves maps in Sivaki dam site. Shear modulus depends on the velocity of shearing wave and density. As the shearing velocity is not the function of humidity and water content of the rock, therefore, the calculated modulus is more applicable. Iso-shear modulus map of A-A' (Figure 18) showed good agreement with iso-shearing velocity map in dam site. The rock observed in southern part of A-A' in iso-shearing velocity map can

be also observed in iso-shear modulus map as well. Similar to elastic modulus, bulk modulus also depends on the velocity of pressure wave, shearing wave and density. As the pressure wave velocity is the function of humidity and water content of the rock, the calculated bulk modulus will be higher than the dry layers. The iso-bulk modulus map of A-A' (Figure 19) showed good agreement with the maps of shearing and pressure velocities in dam site. The rock in the southern part of A-A' and in the northern parts of the section showed higher velocities in pressure and shearing velocities maps. These rocks could be also observed in bulk modulus map.
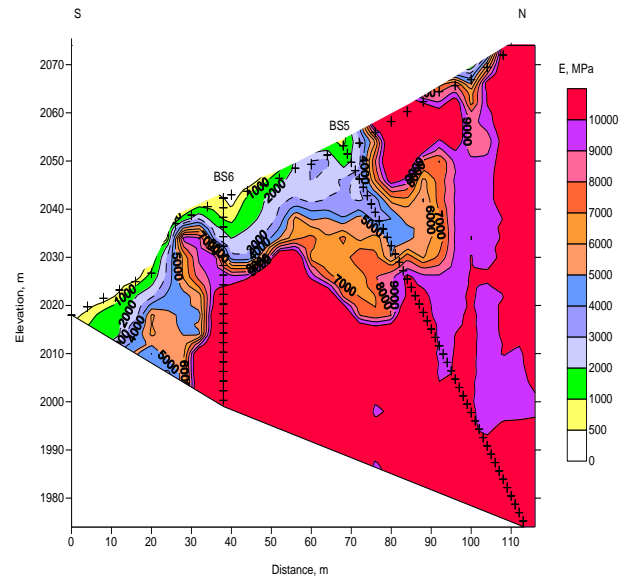

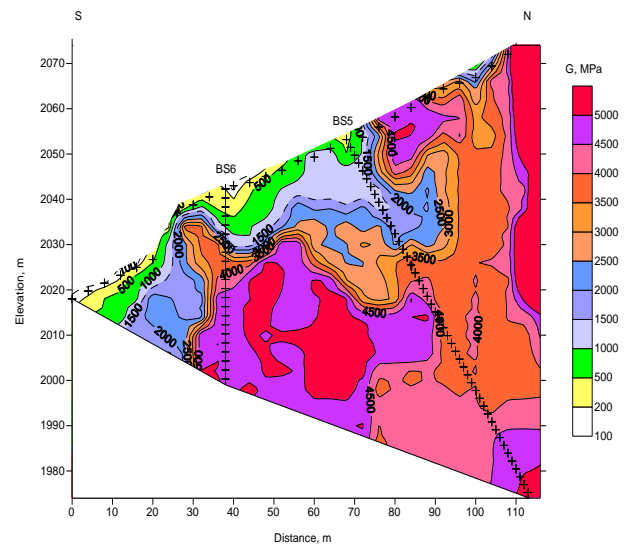**Fig. 17:** The Elasticity Modulus Map of Sivaki Site.

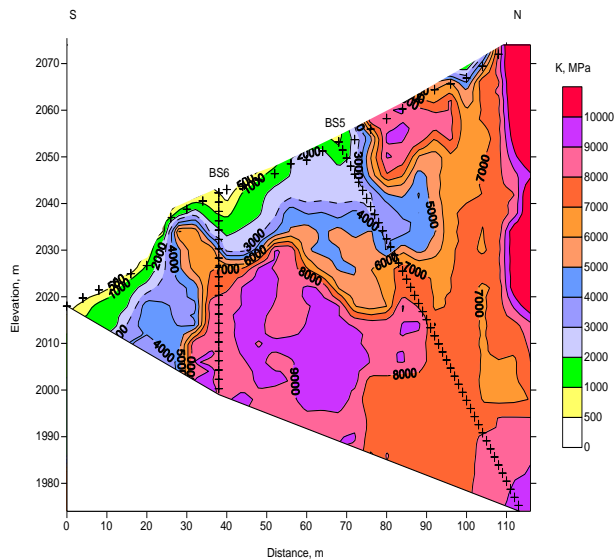**Fig. 18:** The Shear Modulus Map of Sivaki Site.

Fig. 19: The Balk Modulus Map of Sivaki Site.

6. Conclusion

In this study the seismic refraction profiling and seismic tomography methods applied to determine the characterize Sivaki dam site and distinguish the fracture zones, alteration and weathering rocks to evaluation injection and estimation of soil dynamic properties in near to surface. The results of seismic refraction method in the A-A' profile show in the upper part, there is the layer of debris and weathered rocks about 3 to 8 m. In central parts at 4- to 20-m depth, a relatively robust rockmass can be seen. The data of seismic refraction method in the B-B' profile indicated the debris layers and weathered rocks be observed in upper part of this section, the thickness of this layer is about 10 m in southern parts. In central parts of profile, the thickness of debris and weathered rocks reduced to lower than 5 m, in this part, a relatively robust rock can be seen in 4-18 m depth. Geotechnical parameters and dynamic properties were investigated for near-surface soils (up to 30 meter depth) at the right side of Sivaki dam by the help of pressure and shear wave's velocity. The shallow seismic refraction profile have given acceptable information of pressure and shear wave velocities and characteristics of the near surface layers in the dam site. The surface alluvial layers covered the limestone bedrock. Maximum velocity of pressure wave in the site was 3000 m/s corresponding to a region with Lugeon number of 10. In a very small region of the site, Lugeon numbers less than 10 were observed. Results of new studies of Lugeon test for determination of leakage from the foundation and abutments of Sivaki dam site are in good agreement with Lugeon numbers obtained from tomographic seismic methods. Seismic studies showed that rock quality increased with increase of depth but the Lugeon number was more than 10 showing the risk of water leakage even in deeper parts. Based on NEHRP regulation, the Sivaki dam site is preliminarily classified into two site classes B and C. The map does not show iso-Young modulus in A-A' section in contrary to shear and bulk moduli and in general, it shows less similarity with the maps of pressure and shearing waves maps in Sivaki dam site.

References

[1]   H. Motiei, Stratigraphy of Zagros, in A. Hushmandzadeh, (ed). Treatise on the Geology of Iran, Tehran, Geologist Survey of Iran 1993.
[2]   M. Sepehr, J.W. Cosgrove, Structural framework of the Zagros Fold–Thrust Belt, Iran, Marine and Petroleum Geology 21 7 (2004) 829-843. https://doi.org/10.1016/j.marpetgeo.2003.07.006.
[3]   J.S. L'Heureux, M. Long, Relationship between shear wave velocity and geotechnical parameters for Norwegian clays, ASCE J Geotech Geoenviron Eng 21 (2017) 1–20. https://doi.org/10.1061/(ASCE)GT.1943-5606.0001645.

[4]   M. Long, S. Donohue, Characterisation of Norwegian marine clays with combined shear wave velocity and CPTU data, Canadian Geotechnical Journal 47 (2010) 709–718. https://doi.org/10.1139/T09-133.
[5]   T.A. Adedokun, A. Abubakar, Relationship between Hydraulic Conductivity of Rock and Rock Quality Designation of Itisi Multi-Purpose Dam, International Journal on Recent and Innovation Trends in Computing and Communication 2321-8169 (2016) 126-135.
[6]   S.P. Grand, *R.D. Hilst*, S. Widiyantoro, Global seismic tomography: A snapshot of convection in the Earth, GSA Today 7 (1997) 1-7.
[7]   D. Palmer, an Introduction to the generalized reciprocal method of seismic refraction interpretation, Geophysics 46 (1981) 1508-1518. https://doi.org/10.1190/1.1441157.
[8]   D. Palmer, Is visual interactive ray trace an efficacious strategy for refraction inversion? Exploration Geophysics 41 (2010) 260-267. https://doi.org/10.1071/EG09028.
[9]   K.M. Befus, Applied geophysical characterization of the shallow subsurface: Towards quantifying recent landscape evolution and current processes in the Boulder Creek watershed, Master Thesis, Department of Geological Sciences. University of Colorado (2010) 93 p.
[10] J. Attanayake, V.F. Cormier, S.M. Silva, Uppermost inner core seismic structure – new insights from body wave form inversion, Earth and Planetary Science Letters 385 (2014) 49-58. https://doi.org/10.1016/j.epsl.2013.10.025.
[11] R.J. Whiteley, S.B. Stewart, Case studies of shallow marine investigations in Australia with advanced underwater seismic refraction (USR), Exploration Geophysics 39 1 (2008) 34-40. https://doi.org/10.1071/EG08009.
[12] J. Xia, R.D. Miller, B.P. Choon, Estimation of near-surface shear-wave velocity by inversion of Rayleigh waves, Geophysics 64 (1999) 691-700. https://doi.org/10.1190/1.1444578.
[13] D. Farrugia, E. Paolucci, S. D'Amico, P. Galea, Inversion of surface wave data for subsurface shear wave velocity profiles characterized by a thick buried low-velocity layer, *Geophysical Journal International* 206 (2016) 1221–31, https://doi.org/10.1093/gji/ggw204.
[14] D.S. Parasnis, Principles of Applied Geophysics, Published by Chapman & Hall, 1997.
[15] F. Poletto, F. Miranda, Seismic While Drilling: Fundamentals of drill-bit seismic for exploration (Handbook of Geophysical Exploration: Seismic Exploration) Hardcover, Elsevier, 35, 2004.
[16] J. Wong, Crosshole seismic tomography across a masonry dam: Proc. SPIE 2457, Nondestructive Evaluation of Aging Structures and Dams 58 (1995).
[17] A.L. Imhof, C. Calvo, J.C. Santamarina, Seismic data inversion by cross-hole tomography using geometrically uniform spatial coverage, Revista brasileira de Geofʹisica 28 (2010) 79-88. https://doi.org/10.1590/S0102-261X2010000100006.
[18] Y. Zaslavsky, A. Shapira, M. Gorstein., N. Perelman, G. Ataev, T. Aksinenko, Questioning the applicability of soil amplification factors as defined by NEHRP (USA) in the Israel building standards, Natural Science 4 (2012) 631-639. https://doi.org/10.4236/ns.2012.428083.
[19] S.L.M. Miller, R.R. Stewart, Effects of lithology, porosity and shaliness on P- and S-wave velocities from sonic logs, Can. J. Expl. Geophys 26 (1990) 94-103.
[20] R.H. Tatham, Vp/Vs and lithology geophysics, Geophysics 47 (1982) 336 – 344. https://doi.org/10.1190/1.1441339.
[21] S.L.M. Miller, R.R. Stewart, The relationship between elastic-wave velocities and density in sedimentary rocks, A proposal, CREWES Research Report 10 (1994) 260-273.
[22] National Earthquake Hazards Reduction Program (NEHRP), recommended provisions for seismic regulations for New Buildings and Other Structures, Building Seismic Safety Council (BSSC) for the Federal Emergency Management Agency (FEMA 450), Washington, Part 1: Provisions 2003.
[23] S.N .Domenico, Rock lithology and porosity determination from shear and compressional wave velocity, Geophysics 49 (1984) 1188-1195. https://doi.org/10.1190/1.1441748.
[24] C.C. *Potter,* R.R. Stewart, *Density predictions* using Vp and Vs sonic logs, CREWES Research Report 10 (1998) 1-10.
[25] J.E. Nafe, C.L. Darke, Physic properties of Marine sediment, Interscience publishers 3 (1963) 794-815.
[26] G.H.F. Gardner, L.W. Gardner, A.R. Gregory, Formation velocity and density the diagnostic basic for stratigraphic traps, Geophisics 39 (1974) 770-780. https://doi.org/10.1190/1.1440465.

[27] N. Barton, Rock Quality, Seismic Velocity, Attenuation and Anisotropy. CRC Press Book, 2006. https://doi.org/10.1201/9780203964453.

[28] Comité National Français, La deformabilite des massifs rocheux. Analyse ET comparaison des resultants, Int Congress on Large Dams (ICOLD Paris) Q28 (1964) 287-299.

[29] Y. Sharghi, H. Siahkoohi, F. Alinia, P, Moarefvand, Estimation of lugeon number at the abatments of Bakhtyari dam using sesmic tomography, Australian journal of basic and applied sciences 2 (2010) 247-285.

[30] A.C. Houlsby, Construction and design of cement grouting: A guide to grouting in rock foundations, John Wiley New York, 1990.

[31] P. Gretener, Summary of the poissons ratio debate 1990-2003, Feature article, CSEG records (2003) 44-45.

[32] P.V. Sharma, Geophisical methods in geology, Elsevier, Oxford, 1978.

[33] W. Lowrie, Fundamentals of geophysics, Cambridge University press, 1997.

[34] P.H. Mott, J.R. Dorgan, C.M. Roland, The Balk modulus and poissons retio of incompressible materials, Sound vibrate 312 (2008) 572-575. https://doi.org/10.1016/j.jsv.2008.01.026.